Hydrobiologia
https://doi.org/10.1007/s10750-023-05273-9

PRIMARY RESEARCH PAPER

Infection prevalence, intensity, and gill coverage by the parasitic flatworm, *Bdelloura candida*, in the American horseshoe crab (*Limulus polyphemus*)

Christopher J. Brianik · Justin Bopp · Camilla Piechocki · Nancy Liang · Sabrina O'Reilly · Robert M. Cerrato · Bassem Allam

Received: 12 January 2023 / Revised: 20 May 2023 / Accepted: 24 May 2023

Abstract Parasitic infections can have profound implications on host fitness, yet there is minimal information on parasites of the American horseshoe crab (*Limulus polyphemus)*, a species that has experienced recent population declines. Therefore, we aimed to quantify the prevalence, intensity, and gill surface area coverage of the ectoparasite *Bdelloura candida* in adult ($n=58$), sub-adult ($n=7$) and juvenile ($n=32$) horseshoe crabs (HSCs) collected from coastal waters of Long Island, NY in 2019 and 2022. Sub samples of horseshoe crab gill tissue (10%) were collected from live specimens and *B. candida* cocoon intensities from individual lamellae were enumerated microscopically. *B. candida* was present in all adult and sub-adult crabs (100%), whereas juveniles exhibited 6.2% prevalence. 4.0–94.0% of gill lamellae harbored cocoons, with intensities ranging from 0 to 805 cocoons per sub sample. Cocoon covered between 0.06%–14.51% of the gill sub sample surface area, with higher cocoon intensities observed in the ventral-most gill quartiles relative to the dorsal-most regions. Sex was strongly supported as a primary driver behind *B. candida* infection intensities with adult females harboring higher intensities. These results provide novel insight into *B. candida* infection dynamics across HSC demographics, but further research is necessary to quantify the physiological impacts of the infection on *L. polyphemus.*

Keywords Parasitology · Host-parasite interactions · Helminths · Gills · Benthic invertebrate · Image analysis

Handling editor: Iacopo Bertocci

Supplementary Information The online version contains supplementary material available at https://doi.org/10.1007/s10750-023-05273-9.

C. J. Brianik (✉) · J. Bopp (✉) · C. Piechocki · N. Liang · S. O'Reilly · R. M. Cerrato · B. Allam
School of Marine and Atmospheric Sciences, Stony Brook University, Stony Brook, NY 11790, USA
e-mail: Christopher.Brianik@stonybrook.edu

J. Bopp
e-mail: boppjust@gmail.com

S. O'Reilly
Marine Division, Cornell Cooperative Extension of Suffolk County, Riverhead, NY 11901, USA

Introduction

The American horseshoe crab (HSC), *Limulus polyphemus* (Linnaeus, 1758), is an iconic marine arthropod species that has persisted for > 100 million years (Rudkin et al., 2008) and plays critical ecological roles in coastal marine systems from Maine, USA to the Yucatan peninsula in Mexico (Botton, 2009; Smith et al., 2017). These ecological roles include bioturbation (sediment irrigation), structural habitat for epibionts, predation on marine bivalves and benthic macrofauna (Botton and Ropes,

Published online: 30 June 2023

1987; Botton et al., 2003a), while also serving as a critical food source for migratory shorebirds, such as the endangered red knot, (*Calidris canutus rufa;* Linnaeus, 1758) (Tsipoura & Burger, 1999; Smith et al., 2017). In addition to their numerous ecological roles, HSCs are an important human health and economic resource. The hemolymph (blood) of HSCs is collected by biomedical companies to extract a unique compound, *Limulus* amebocyte lysate, that is used to detect the presence of endotoxins from gram-negative bacteria in human medical supplies, and this practice has resulted in a threefold increase (currently 500,000 HSCs) in biomedical harvest since the 1980s (Eyler, 2015; Smith et al., 2017). Moreover, roughly 1–2 million crabs are exploited annually for bait in the whelk and eel fishery throughout the US East Coast (ASMFC, 2019). Exploitation from these industries has been perceived to be the primary contributor towards their recent coastwide declines, which has led to their "Vulnerable" conservation status in the US (Smith et al., 2016). Despite the current management interest, the impacts of biotic stressors (e.g., parasite infections) on HSC fitness and population dynamics have rarely been addressed, as management strategies have primarily focused on direct anthropogenic exploitation.

Parasites are ubiquitous in nature with most wild animals harboring at least a low intensity infections, with the prevalence and intensity frequently increasing with size, age, and density of the host (Zelmer et al. 1998). Parasites are capable of influencing numerous aspects of their host's biology including survival, fecundity, population cycles, and behavior (Ebert et al., 2000; Tompkins & Begon 1999; Hudson et al., 1998; Lehmann 1993; Poulin, 2010) with cascading impacts on the entire ecosystem. Although variable between host species, low parasite intensities are typically well tolerated by a host (e.g., pinworm in humans) (Lehmann 1993; Stjernman et al., 2008); however, intense infections often result in adverse outcomes for a host. For instance, infections by the roundworm *Ascaris lumbricoides* Linnaeus, 1758 in the human intestine are considered to be mildly symptomatic, but the mere presence of numerous worms can cause blockages leading to indirect intestinal damage (Despommier et al., 2020). Similar observations have been made in aquatic animals, as many Monogenea (commonly observed ectoparasites of fish and amphibians) have been observed to damage their host not through resource exploitation, but via their attachment organs that penetrate the epithelial layer leading to excess mucus production and inflammation (Whittington, 2005). Moreover, Monogenea infecting gill tissue have been demonstrated to adversely impact survival of aquatic organisms exposed to oxygen-poor conditions (Molnar, 1994), with oxygen carrying capacity reduced up to 50% in crustaceans and fish (Taylor et al., 1996). Although several internal parasitic symbionts (trematodes and nematodes) have been recorded in HSCs (Leibovitz & Lewbart, 2003), the basic information on external parasites (i.e., prevalence, intensity and associated physiological impacts) such as the flatworm, *Bdelloura candida* (Girard, 1850), are not well established in the literature.

Bdelloura candida is a 2 cm long triclad flatworm that is an obligate parasite of the American horseshoe crab. Adult worms are primarily located on the walking appendages and book gills, while the cocoons are attached on the inner surface of the gill lamellae by means of an endplate, an appendage akin to an anchor (Sluys, 1989). Histological sampling has revealed that cocoons of triclad worms can cause necrosis of surrounding gill tissue (Groff & Leibovitz, 1982; Leibovitz & Lewbart, 2003). Few studies have quantified the extent of *B. candida* infection prevalence or intensity, with no information pertaining to host traits related to infection data. A maximum of 50 *B. candida* cocoons have been documented on HSC lamella in previous studies, but small sample sizes have resulted in limited inference of infection dynamics on HSC populations (Leibovitz & Lewbart, 2003). *B. candida* have also been observed throughout the entire HSC geographic range (Mexico to Maine, USA) (Riesgo et al., 2017). Outside of these studies, information pertaining to *B. candida* prevalence, intensities, and their coverage on HSC gills, particularly across ontogeny, remains limited.

In this study, juvenile, sub-adult, and adult HSCs were sampled from an estuary along the south shore of Long Island, New York, to better understand *B. candida* infection dynamics. The primary objectives of this work were to: (1) quantify *B. candida* intensity and prevalence across HSC demographics (age groups and sex) and (2) investigate intrinsic (size, sex) factors that explain *B. candida* intensities in HSCs, and quantify the percentage of gill tissue occupied by *B. candida* cocoons. We also assessed the

infection intensity across the vertical gill space (ventral to dorsal) and between the central-mitochondrial rich area (CMRA) vs. peripheral mitochondrial-poor area (PMPA) to determine if infection intensity was random (homogenous) or aggregated (heterogenous) among different gill surface regions (Hans et al., 2018). This study provides novel insight into the infection dynamics of *B. candida* on HSCs and could serve as the basis of monitoring ectoparasite infection in wild HSC populations in tandem with other surveys, such as the U.S. East Coast citizen science HSC tagging survey that has been established by the United States Fisheries and Wildlife Service since 2002 (Bopp et al., 2019).

Materials and methods

Sample collection

Samples used in this study are summarized in Table 1. Adult HSCs were collected at Pikes Beach, Moriches Bay, Long Island, NY (40.77°N, − 72.71°W; Fig. 1) in June of 2019 ($n = 29$) and 2022 ($n = 30$). The 2019 sample was collected haphazardly while the 2022 sample was obtained from a local bait fisherman and only used for calculation of prevalence and intensity. Sampling in nearshore areas for 2020 and 2021 was not possible due to the COVID-19 pandemic. In 2019 juvenile crabs ($n = 30$) between instars 8–10 (prosomal width range 41.4–57.9 mm) (Sekiguchi, 1988; Carmichael et al., 2003) were also haphazardly collected by hand along a 500 m transect at the water's edge (< 0.5 m depth). Juvenile crabs were then transported back to the lab where they were euthanized using an overdose of Tricaine-S (MS-222) and frozen at − 20 °C for long term storage. All adults (prosomal width range 188.0–283.0 mm) were collected from the intertidal zone (~ 0.5–1 m deep) shortly before high tide and were temporarily placed

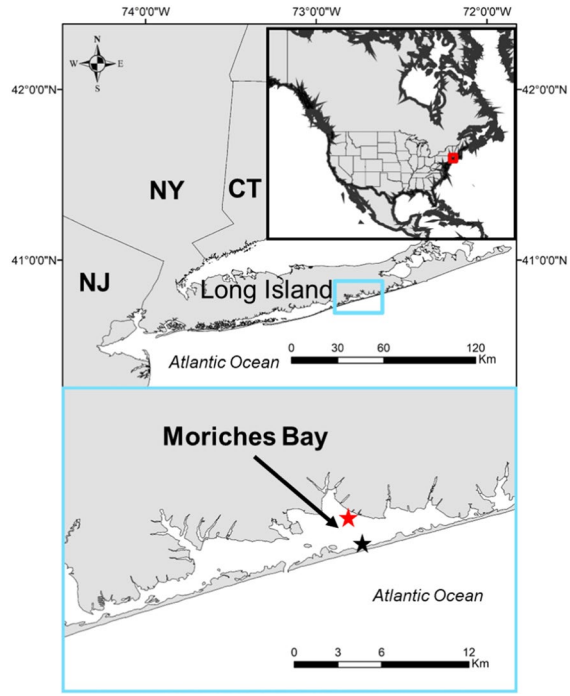

Fig. 1 Map of Moriches Bay in Long Island, NY, USA. The black star represents Pike's beach, the intertidal sampling location for juvenile and adult crabs 2019. The red star denotes the trawl survey location where sub-adult crabs were opportunistically sampled in 2020

Table 1 Summary of samples used in this study

Location	Sample size	Year	Lethal or nonlethal	Age class	Prosomal width range (mm)	Sample collected
Pikes Beach Moriches bay	29	2019	Nonlethal	Adult	188.0–283.0	Gill subsample and adult worms
Pikes Beach Moriches bay	30	2019	Lethal	Juvenile	41.4–57.9	Entire crab
Trawl survey Moriches bay	7	2020	Nonlethal	Sub-adult	113–179	Nonlethal visual inspection
Trawl survey Moriches bay	2	2020	Nonlethal	Juvenile	40.5–57.2	Nonlethal visual inspection
Pikes Beach Moriches bay	30	2022	Lethal	Adult	230.0–390.0	Entire book gill

in fish totes filled with ambient seawater. Sex, prosomal width, and weight were recorded for every individual. Sex was determined by the presence of modified pedipalps, weight was measured using a Pesola (Schindellegi, Switzerland) 10 kg (±0.3%) spring scale, and prosomal width was measured to the nearest millimeter using Vernier calipers. The gills of adult crabs from 2019 were subsampled by removing the upper-right portion of book gills (nonlethal), which constituted approximately 10% of their gills (Fig. 2), while the entire book gill (lethal) was collected from specimens during the 2022 sampling to determine the relationship between *B. candida* infection patterns in gill subsamples as compared to that in the entire gill space. Both 2019 gill samples and *B. candida* samples were individually stored in 70% ethanol to be counted at a later time. After sample collection, adult crabs from the 2019 sample were released immediately back to the water.

In addition, opportunistic samples of *L. polyphemus* were obtained from a trawl survey in September–October 2020 from the muddy habitat (~2 m depth) of Moriches Bay (40.79°N, − 72.71°W). This sample consisted of 2 juveniles (instars 9 & 10; prosomal width range 40.5–57.2 mm) and a subadult cohort ($n=7$; instars 14–18; prosomal width range = 113.0–179.0 mm). Gill samples from these crabs were not removed, but instead were carefully examined for the presence of *B. candida* cocoons and adult worms to determine if any differences in *B. candida* prevalence were observed among crabs residing on the continental shelf and in local estuaries.

To obtain *B. candida* adult intensity in a standardized format, forceps were used to remove *B. candida* worms from the book gills and legs over a timed 5 min period immediately following the physical measurements of the 2019 adult crabs. This served as a proxy for catch-per-unit-effort (CPUE). This timed approach was implemented for two reasons: (1) every adult flatworm could not be accurately removed from the adults by hand or by brief freshwater rinses and (2) to minimize the desiccation stress to the animals during sampling. All adult worms collected during each 5 min sampling period were stored in 30 ml of 70% ethanol in 50 mL Falcon conical centrifuge tubes and were processed later in the lab. Prevalence of *B. candida* was determined by tallying the presence of either adult worms or cocoons on HSC gill tissues or other appendages. Population prevalence was determined as the percentage of individuals that were infected by *B. candida.*

B. candida intensity measurements

To measure adult flatworm intensity, collected adult flatworms were counted and recounted under a dissecting microscope by three readers. Samples were randomly chosen, and readers were blinded from previous recorded intensities in the same sample to minimize bias. The final intensity count was determined if two or more observers had the same

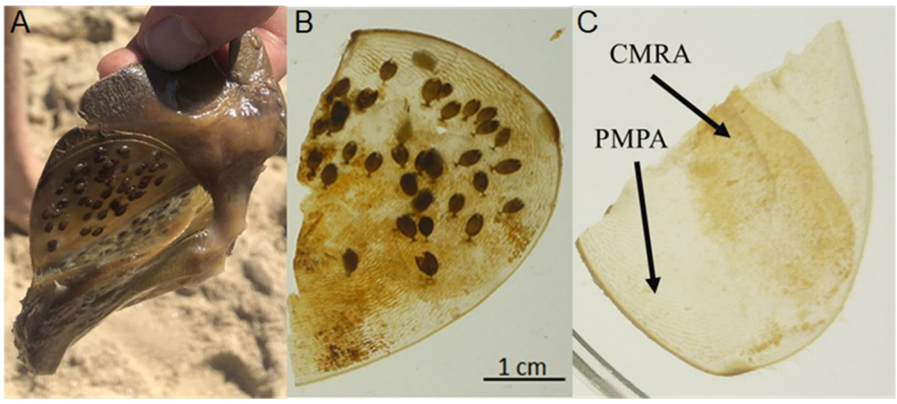

Fig. 2 **A** Book gill (10% of the total gill) removed from an adult horseshoe crab, in which the ventral most lamellae (in the 4th quartile) is heavily infected with *B. candida* cocoons. **B** An individual gill lamella (from the 4th quartile) with *B. candida* infection (> 25 cocoons). **C** The central mitochondria-rich area (CMRA) is located within the mid-section of the lamellae and has a darker pigmentation relative to the more transparent peripheral mitochondria-poor area (PMPA)

intensity counts. If all counts differed between readers in a sample, a fourth reader counted the sample to finalize intensity based on agreement with another reader. Intensity was defined as the total count of adult *B. candida.*

To measure the intensity of *B. candida* cocoons, each individual lamella was removed from the book gill subset. *B. candida* cocoons were enumerated under the dissecting microscope for each gill lamella in each gill sample subset. Lamellae can be divided into two sections, the central mitochondria-rich area (CMRA) which is important for ammonia excretion and/or acid–base regulation and the less ion-leaky peripheral mitochondria-poor area (PMPA) (Hans et al., 2018). The intensity of cocoons present on the CMRA and the PMPA regions of the lamellae was also enumerated. Figure 2 visually illustrates CMRA and PMPA delineations.

Gill and cocoon surface area preparations and measurements

After measuring cocoon intensity, each lamella from the 2019 sampling was placed on a lightbox with a ruler and photographed using a digital Panasonic LUMIX DMC-T380 waterproof camera. Every gill subset was sampled from the ventral to the dorsal side. However, lamella measuring less than 1 cm in diameter (typically the first few in the book gill) at its widest point were not photographed as they were not observed to harbor any infections and their small size contributed little to total respiratory surface area. One gill sample deteriorated during processing and could not be analyzed.

To measure the proportion of gill surface area covered by the cocoons, cocoon area and gill lamella surface area were measured using ImageJ (version 1.8.0) software (Schneider et al., 2012). The local threshold tool was used to automatically detect and measure the surface area of the cocoons against the lamella, which limited human error. In cases where the color threshold inadequately distinguished cocoons or lamella from each other, manual measurements were made in ImageJ. Average cocoon size was determined by randomly sampling 100 cocoon measurements across all individual adult crabs.

Histological analysis

Gill samples (~2 cm x 1 cm × 0.5 cm; $n = 6$) from HSCs, not used in the other analyses, were removed and placed in histo-cassettes then fixed in 10% buffered formalin, and embedded in paraffin wax. Sections (~5 µm) were mounted on slides and stained with Harris's haematoxylin and eosin. Slides were visually inspected for any signs of pathology, such as inflammation, necrosis or encapsulation.

Statistical analyses

To determine if gill subsamples were representative of cocoon intensities in the entire gill, all cocoons were counted on 28 HSCs (2 samples were damaged during collection) from the 2022 sample (15 females, and 13 males) and a linear regression model with total cocoon count versus cocoon intensities from the subsamples was constructed. Prior to fitting the linear model, a Shapiro–Wilk test was used to test for normality.

A generalized linear model (GLM) was employed to determine which intrinsic factors explained the most variance behind cocoon intensity in adult HSC gill tissues. *B. candida* prevalence and cocoon intensity data were collected on both 2019 and 2022 samples, but only crabs sampled in 2019 were included in the GLMs because gill surface area and adult flatworm intensity were not collected from the 2022 samples. The response variable was cocoon intensity and the explanatory variables were adult flatworm intensities, total gill surface area, and sex in the GLM. Prior to constructing the model, cocoon intensity data was fit to Poisson and negative binomial error structures and each distribution was compared by Akaike's information criterion (AIC) in the *fitdistrplus* R package (Delignette-Muller & Dutang, 2015; R version 4.0.2, R Core Development Team, 2020) to determine the most appropriate error structure given the data. In all GLMs, multicollinearity between the explanatory variables was assessed by calculating the variance inflation factor (VIF) in the *Performance* R package (Lüdecke et al., 2020). Variables with a VIF greater than 5 were removed from the GLM, as VIFs above 5 are considered to be moderately or strongly correlated with each other and strong correlations between one or more predictor variables can lead to erroneous and biased estimates (Gareth et al.,

2013). Given that size (prosomal width) is a sexually dimorphic trait in all HSC populations (Smith et al., 2009; Bopp et al., 2019) and it had the largest VIF (3.43, 95% CI 2.26–5.69) in both GLMs, size was not included as an explanatory variable in the global models for cocoon and adult flatworm intensity candidate sets. Outside of size, other explanatory variable VIFs were < 3 and were therefore, not removed from the global model prior to fitting and model selection analysis. The fit of all possible GLM model variants was assessed with the dredge function in the *MuMin* R package (Barton & Barton, 2015). Inference was drawn from models within each GLM candidate set using the small sample size corrected Akaike Information Criteria (AICc) and AIC weights (Burnham & Anderson, 2002). Model variants with ΔAICc < 2 and AIC weights > 0.10 were considered to have moderate support (Burnham & Anderson, 2002).

A separate GLM was constructed to examine the relationship between adult flatworm intensity and the explanatory variables total gill surface area, sex, and HSC size. Similar to the other GLM, negative binomial and Poisson error distributions were fit to adult flatworm intensity data and were assessed with AIC. As aforementioned, the multicollinearity analysis was repeated, eliminating size, and model selection was again carried out using the dredge function.

To determine if intensity was homogenous or aggregated across gill tissue space (ventral to dorsal sections), each individual crab's gill subsets were split into four quartile groups and the total cocoon intensity for each gill quartile was summed. Quartile groups were chosen because of variability in the number of lamella present amongst individual HSCs. To determine if cocoon frequencies differed among quartile groups, a chi-square test of frequencies was employed. A linear regression test was also employed between the quartile group with the highest cocoon intensity (4th quartile) and the total cocoon intensity across gill samples to determine if the most infected gill quartile could serve as a relative proxy of overall cocoon infection intensity.

To determine if *B. candida* cocoons were spaced randomly or preferentially across mitochondrial regions of the lamellae in infected individuals, cocoon frequencies among on the CMRA regions vs. PMPA regions were compared with a chi-square test. Each of these regions can be assessed visually given their contrasting pigmentation on gill lamellae (Fig. 2C; Hans et al., 2018). To understand how frequencies may be associated with different sizes of the mitochondrial regions, CMRA regions of 100 lamellae were randomly measured using ImageJ. PMPA surface area was then measured from the subtraction of CMRA from the total area same lamella of the CMRA measurement.

Results

Prevalence and intensity

From the HSCs collected in June of 2019 and 2022, *B. candida* infections (both adult worms and cocoons) were present in 100% of adult gill samples ($n = 59$), while only 1 juvenile (instars 8–11) from the 2019 collection date ($n = 30$) was observed to harbor any signs of infection (3 cocoons). The opportunistic samples procured in October of 2020, showed a similar pattern with 100% of subadults ($n = 7$; instars 16–18) being observed to have either adult worms and/or cocoons. The two juveniles obtained in 2020 (instars 9–11) were the least infected from this time point with one having no signs of infection and the other having a single cocoon. From the infected adult crab sub samples, both cocoon intensity and adult worm counts varied considerably, as intensities of cocoons and flatworms ranged from 28 to 805 ($\underline{x} = 198 \pm 26$ SE) and 5 to 196 ($\underline{x} = 58 \pm 9$ SE), respectively. Adult female HSCs had an average of 245 ± 34 SE cocoons; whereas, males had a lower average cocoon intensity ($\underline{x} = 43 \pm 10$ SE cocoons). Cocoon intensities were also lower in 2022 ($\underline{x} = 86 \pm 23$ SE) compared to 2019 ($\underline{x} = 259 \pm 40$ SE) (Wilcoxon rank sum test, $n = 58$, $W = 159$, $P < 0.001$). Average *B. candida* cocoon intensities ranged from 0.4 to 12.2 ($\underline{x} = 3.2 \pm 0.50$ SE) per gill lamella. Total number of gill lamellae (> 1 cm diameter) also varied between crabs with counts ranging from 53 to 125 ($\underline{x} = 91 \pm 3$ SE). Cocoon coverage differed by two orders of magnitude among adult crabs, covering between 0.10% and 14.5% ($\underline{x} = 2.3\% \pm 0.6\%$ SE) of total gill surface area (based on gill subsamples) (Fig. 3). The proportion of cocoons occupying the CMRA regions ranged from 0.05 to 0.53 ($\underline{x} = 0.21 \pm 0.02$ SE) in infected adult HSCs (Fig. 4).

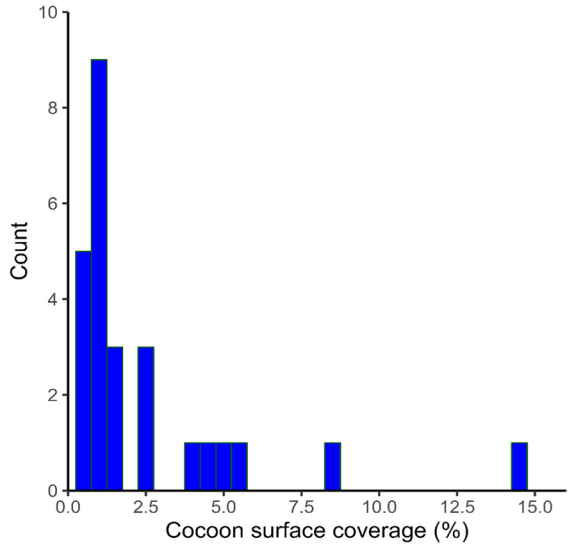

Fig. 3 Histogram of the percentage of gill surface area covered by cocoons in infected adult horseshoe crabs ($n = 29$)

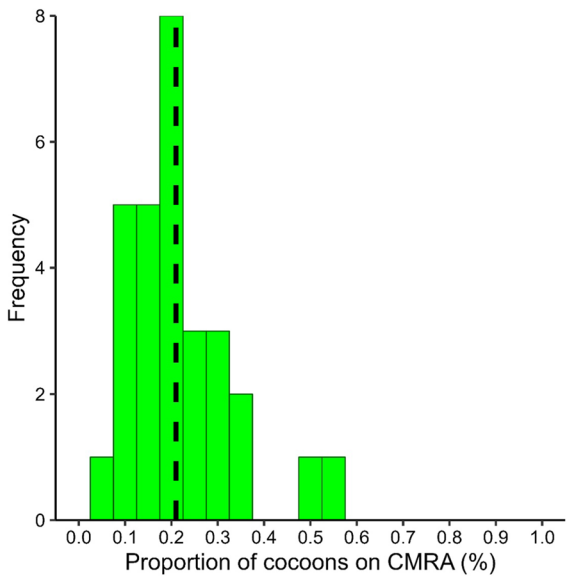

Fig. 4 Histogram showing the proportion of *B. candida* cocoons within the central mitochondrial-rich area in the gill lamellae ($n = 29$). Vertical line denotes the mean proportion of cocoons on CMRA (0.21 ± 0.02 SE)

Microscopic analysis

Histological observations showed healthy HSC leaflets consisted of parallel lamellae connected via pillar cells, with vascular lumina containing hemolymph filling space between the pillars (LaDouceur et al., 2019; Fig. 5A). The dorsal tips of the leaflets were covered in a thickened proteinaceous matrix, which also covered the epithelium of the leaflets, albeit not as thick as the blunted dorsal tips (Fig. S1A). Superficial mats of bacteria and algae also frequently covered sections of gill epithelium but are likely nonpathogenic due to lack of infiltration and were not observed to cause any inflammation (LaDouceur et al. 2019; Fig. 5A). In infected HSC leaflets, *B. candida* cocoons were elliptical in shape with an anchor shaped protrusion extending from one side, and they were attached to the lamellae epithelium via a cement-like excretion that surrounded

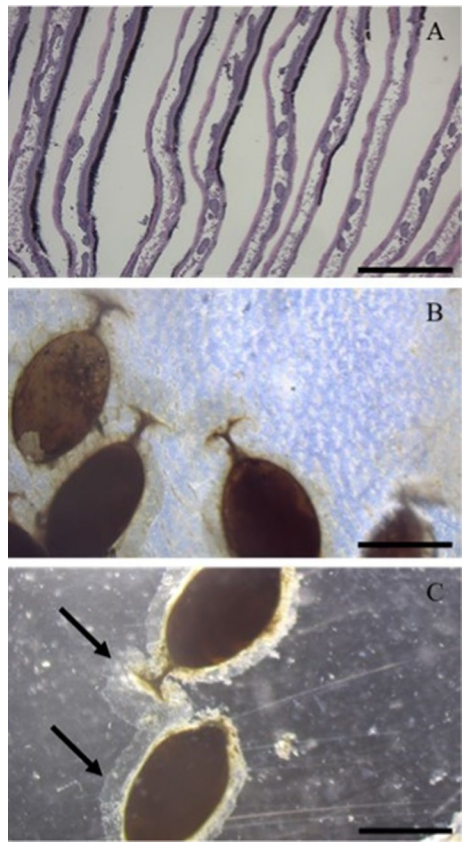

Fig. 5 **A** Normal histology of gill lamella not impacted by *B. candida* cocoons. Non pathogenic biofilms (black) are present on the acellular layer of the chitinous epithelium (scale bar = 500 µm). **B** *B. candida* attached to a lamellae (scale bar = 1 mm). **C** *B. candida* removed from a lamellae with adhesion substance surrounding the cocoons and pointed out with arrows (scale bar = 1 mm)

the cocoon body and the anchor (Fig. 5B–C). After randomly sampling 100 single cocoons, the average cocoon area was 3.37 ± 0.07 SE mm^2. Surface defects that impacted the organization of epithelial tissue, disrupting and breaking the parallel chitinous layers of the lamellar structure, were observed in histology sections of infected lamellae with melanization frequently observed on the outer layer of these lesions (Fig. S1C, D). Hemocyte nodules were frequently observed in the vascular lumen of the lamellae causing hemocyte aggregation, encapsulation and inflammation (Fig. S1B–D).

Generalized linear model: cocoon intensity

Linear models were used to assess if gill subsamples were reflective of total cocoon intensities and to evaluate what host factors were associated with infection intensity. Linear regression models demonstrated a moderately positive relationship between total gill cocoon intensities and intensities in the gill subsamples ($R^2 = 0.42$, $P = < 0.01$, $n = 28$). The negative binomial distribution was chosen for the cocoon intensity GLM, as the AIC was lowest for the negative binomial distribution relative to the Poisson distribution (ΔAIC 4673.7). Therefore, a negative binomial family error structure was used in the candidate model set. The GLM model selection process revealed that three out of 8 model variants had moderate support (cumulative AIC weight > 0.88) according to ΔAIC values and AIC weights (Table 2). Adult flatworm intensity was supported in all three models, but the top model had support for gill surface area and sex (Table 2). The evidence ratio of the top model relative to model three was ~ 1.9 (Table 2), suggesting that the top model is nearly 2 times more probable than model 3. However, model selection uncertainty was present between the top three models given ΔAIC < 2 (Table 2).

Generalized linear model: adult worm intensity

The negative binomial distribution was used as the family error structure in the GLM given it was a better fit (AIC = 293.9) compared to the Poisson distribution (AIC = 1166.2). Model selection revealed that 3 out of 4 possible model variants relating adult flatworm intensity to covariates had moderate to strong support (Table 3) with model selection uncertainty present. The top model only included sex and had an evidence ratio of ~ 3 relative to models 2 and 3, indicating this model is nearly 3 times more probable compared to the other models. Model support for gill surface area (models 2 and 3) was weaker compared to sex in terms of affecting adult flatworm intensities (Table 3).

Table 2 Candidate model results for generalized linear model (GLM) for the cocoon intensity of adult horseshoe crabs after model fitting with the dredge package in R

Model Number	Model	NP	Log likelihood	AICc	ΔAICc	Akaike weight
1	Cocoon intensity ~ adult intensity + gill surface area	4	− 181.5	372.8	0	0.37
2	Cocoon intensity ~ adult intensity	3	− 183.1	373.1	0.3	0.32
3	Cocoon intensity ~ adult intensity + sex	5	− 180.7	374.0	1.2	0.20
4	Cocoon intensity ~ adult intensity + sex + gill surface area	6	− 180.1	375.9	3.1	0.08
5	Cocoon intensity ~ gill surface area	3	− 186.6	380.2	7.4	0.01
6	Cocoon intensity ~ sex	4	− 185.4	380.4	7.6	0.01
7	Cocoon intensity ~ sex + gill surface area	5	− 184.0	380.7	7.9	0.01
8	Cocoon intensity ~ 1	2	− 189.8	384.1	11.3	0.00

A total of 8 possible model combinations were assessed, but only models with moderate support (Akaike weight > 0.10 and ΔAICc < 2) are shown here (see Methods) and are ranked by AICc. The cumulative Akaike weight between these models comprised 0.88. The global model included sex, adult worm intensity, and gill surface area, as explanatory variables with cocoon intensity set as the response variable. NP represents the number of parameters. The negative binomial distribution was the family error structure used in the GLM, as AIC was lower for the negative binomial distribution relative to the Poisson distribution (ΔAIC 4673.7)

Table 3 Candidate model results for generalized linear model (GLM) for the adult worm intensity of adult horseshoe crabs after model fitting with the dredge package in R

Model Number	Model	NP	Log likelihood	AICc	ΔAICc	Akaike weight
1	Adult worm intensity ~ sex	4	− 140.7	291.2	0	0.56
2	Adult worm intensity ~ gill surface area + sex	5	− 140.5	293.6	2.4	0.17
3	Adult worm intensity ~ gill surface area	3	− 143.4	293.8	2.6	0.15
4	Adult worm intensity ~ 1	2	− 144.9	294.4	3.2	0.12

A total of 4 possible model combinations were assessed, but only models with moderate support (Akaike weight > 0.10) are presented and are ranked by AICc. The cumulative Akaike weight between these models comprised 0.88. The global model included sex and gill surface area as explanatory variables with adult intensity set as the response variable. NP represents number of parameters. The negative binomial distribution was used as the family error structure in the GLM given it was a better fit (AIC = 293.9) compared to the Poisson distribution (AIC = 1166.2)

Spatial patterns of cocoon intensities

Cocoon infection intensity differed among gill lamellae quartiles (Chi-square test; $\chi^2 = 1445.9$, DF = 84, $N = 29$, $P < 0.001$). Gill quartile 4 (ventral-most) had higher cocoon intensities relative to all other gill quartiles (Fig. 6). Gill quartile 4 exhibited a strong positive relationship (Spearman rank correlation; $\rho = 0.96$, $P<0.001$) with overall infection intensity in the gill subsample (Fig. 7).

Cocoon intensity on CMRA vs. PMPA

Cocoon intensities differed between the CMRA and PMPA regions (Chi-square test; $\chi^2 = 408$, DF = 27, $N = 29$, $P < 0.001$). The average proportion of cocoons occupying the CMRA region of gill lamellae was lower ($\underline{x} = 21.0\% \pm 2.0\%$ SE) compared to the PMPA region. Out of the 100 random lamellae measurements, the average proportion of the CMRA region vs. total gill area was $30.6\% \pm 0.6\%$ SE.

Discussion

This study demonstrates that *B. candida* infections are highly prevalent among adult HSCs, and that the cocoons of this parasite are capable of occupying a considerable amount of gill surface area (> 10%). To our knowledge, the only previous studies evaluating

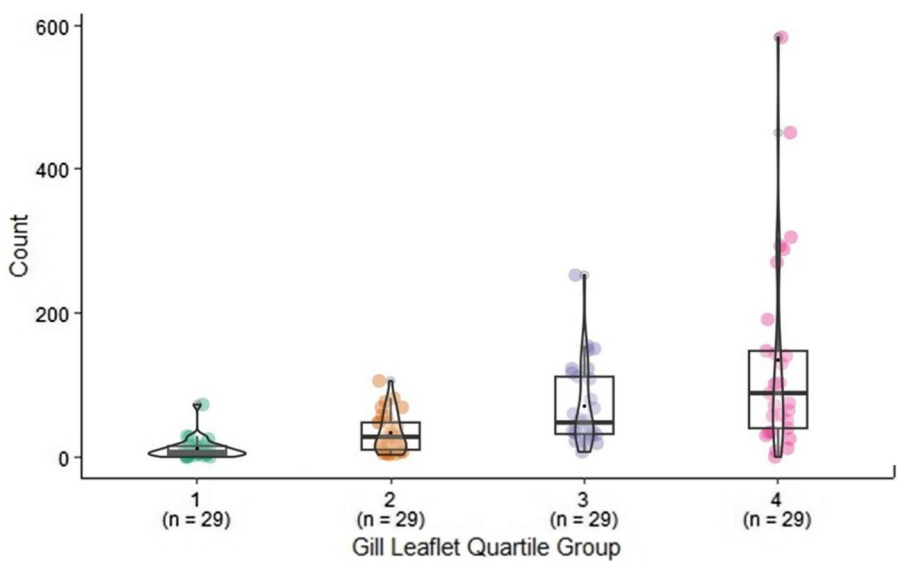

Fig. 6 *B. candida* cocoon intensity for four gill lamellae quartile groups. The first quartile represents the dorsal-most gill lamellae; in contrast, the fourth quartile represents the ventral-most gill lamellae. Black dots represent each individual horseshoe crab's cocoon intensity in each gill lamellae quartile. Chi-square test revealed differences in cocoon frequencies among quartile groups ($n = 29$ per group, $\chi^2 = 1445.9$, DF = 84, $P < 0.001$)

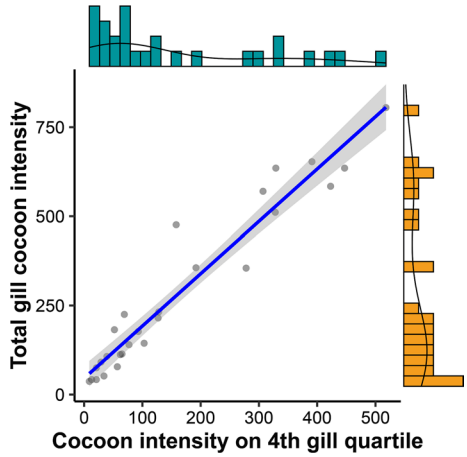

Fig. 7 Scatter plot of cocoon intensity from the 4th quartile of gill (ventral-most) leaflets ($n=27$) vs. gill subsample cocoon intensity collected from the 2019 adult samples. The blue bars show a histogram displaying the frequency of cocoon intensities infecting the 4th-gill quartile. The orange bars show a histogram displaying the frequency of cocoon intensities in the entire gill subsample. The lines that overlay the histograms represent the probability density distribution of the data. The Spearman rank correlation results were: $\rho=0.96$ and $P<0.001$. Standard error is represented by grey shading

B. candida infection intensities demonstrated that adult HSCs had 400–800 (average = 575, $n=4$) cocoons across their entire gill area (Pearse 1949) and are capable of having > 50 cocoons within a single gill lamella (Leibovitz & Lewbart 2003). In contrast, the average *B. candida* intensity was 175 ± 26 in this study within our subsamples (10% of the total HSC gill area) and the average total cocoon count in each crab was 931 ± 137 (2022 only). Interestingly, cocoon prevalence and intensity were not uniform across life history stages, as only 6.2% ($n=2$) of juvenile crabs (instars < 13; 58 mm) had cocoons attached to their gills, whereas all adults and sub-adults were observed to have cocoons and adult worms. Moreover, all cocoon intensities were orders of magnitude higher on adult crabs than juveniles (when present). Ontogenetic shifts in parasite infrapopulations are common, and we demonstrated that both prevalence and infection intensities increased with age in HSCs. However, the mechanisms leading to the observed adult-juvenile dichotomy in *B. candida* prevalence is intriguing, as juvenile (instar groups 8–10) and adult crabs share the same habitat (spawning beaches) during the spring possibly exposing the juvenile crabs to the parasite. The high (100%) prevalence of *B. candida* in adult crabs suggests that *B. candida* is well adapted at colonizing a susceptible host with transmission unlikely to be limiting to juveniles; therefore, these age-group prevalence trends may presumably be a result of behavioral, foraging, or physiological differences between the stages.

A possible explanation for the ontogenetic differences in infection are due to the decrease in molting frequency observed in HSCs as they age. Juvenile HSCs molt several times a year until reaching instar 10 (49.2 mm), after which molting occurs annually until a terminal molt is reached upon sexual maturation (Carmichael et al., 2003; Estes et al., 2015). Following the terminal molt, the accumulation of epibionts on HSCs (slipper snails, barnacles, macroalgae, etc.) are well documented (Walls et al., 2002) with similar dynamics likely to influence the establishment of *B. candida.* Host traits that reduce molting frequency, such as age and egg-bearing, have been associated with increased prevalence and intensity of ectoparasites in other marine anthropods, including Antartic krill, (*Euphausia superba* Dana, 1850) and the American lobster (*Homarus americanus* Milne-Edwards, 1837) (Tarling & Cuzin-Roudy, 2008; Castro et al., 2012). Although molting seems to be a likely mechanism in *B. candida* regulation, it is difficult to test, as the most heavily infected cohort (adults) rarely molt and are difficult to maintain in laboratory conditions in sufficient numbers to test such a hypothesis.

Outside of molting, other phenomena such as HSC behavior, ontogenetic differences in size, physiology and resource use may explain prevalence dynamics across age groups. For instance, it is possible that *B. candida* is sexually transmitted and initiates infection during the extensive copulatory process observed in HSCs in which multiple males may attach to one female for days to months each spring (Brockmann & Penn, 1992). However, the observation of 100% infection prevalence among the sub-adults ($n=7$, instars 16–18) in this study makes this an unlikely scenario, as this age group does not share habitat or engage in mating behavior (Rudloe, 1981). Differences in gill surface area between instars 8–10 and sub-adults/adults may also be a primary factor behind prevalence disparities, as parasite intensity can correlate with increasing body size such is the case with *Lepeophtheirus salmonis* (Krøyer, 1837) infecting Atlantic

salmon (*Salmo salar* Linnaeus, 1758) (Tucker et al., 2002; Drake, 2019), presumably a result of increased surface area reducing space competition among conspecific ectoparasites. The body size argument may also explain why HSC sex was a contributing factor in *B. candida* infection rates because adult females are larger than males (Loveland & Botton, 1992) and thus, females have more available surface area for *B. candida* to reside.

The difference in infection intensities among age groups may partially reflect contrasting foraging behaviors among life history stages and may make the juvenile cohort (< 12 instars) unsuitable for *B. candida* establishment. For example, *B. candida* is believed to indirectly consume food particle remnants from HSC feeding activities (Jennings, 1977). Juvenile crabs (instars < 10) predominantly rely on sedimentary organic matter and meiofauna adjacent to salt-marsh habitats (Botton et al., 2003b); in contrast, older juvenile and adult crabs predominantly forage on larger-bodied prey, such as bivalves and polychaetes (Botton & Ropes, 1987; Gaines et al., 2002). Therefore, the nutritional resources on juvenile HSCs may not be sufficient for *B. candida's* nutritional requirements. However, the theory of *B. candida* foraging on remnants of HSC prey items remains controversial due to chemical analysis indicating that *B. candida* may obtain some nutritional energy directly from HSCs (Lauer & Fried, 1977). The application of modern techniques to assess resource use, such as stable isotope analysis (bulk or compound-specific), could be used to resolve this controversy as it could identify the nutritional resources adult *B. candida* predominantly relies on.

Given that this study emphasized one population of HSC hosts, we cannot state these infection intensity patterns apply to other populations, as other factors such as biogeographic differences in reproduction ratios, environmental conditions, migration patterns, abundance, and size may alter *B. candida* infection dynamics. Bagge et al., (2004) noted that the primary determinant behind infection rate variability for multiple monogenean species' in *Carrasius carassius* (Linnaeus, 1758; the crucian carp) was host population size, presumably due to a required infection density threshold for effective transmission, and thus numbers of hosts were the limiting transmission factor. For HSCs, population densities are the largest in Mid-Atlantic populations (Delaware and Chesapeake Bays) and can be 2–400 times greater than their more temperate or tropical counterparts (James-Pirri, 2005; Mattei et al., 2010; Smith et al., 2009, 2017; Shuster, 1955). In addition, maximum body sizes of HSCs are the greatest in Mid-Atlantic populations (Shuster, 1955). In turn, *B. candida* intensity may contrast between host populations due to both disparate population densities, abundances, and body size differences of *L. polyphemus*. Previous studies have demonstrated that ectoparasite intensities can increase with host body size in a variety of animal species, including chigger parasites on the spiny lizard (*Sceloporus clarkii* Baird and Girard, 1852) (Watkins & Blouin-Demers, 2019), lice on multiple species of woodpeckers (Galloway & Lamb, 2017), and ectoparasitic copepods in *Salvelinus fontinalis* (Mitchill, 1814) (Poulin et al., 1991). Therefore, assessing *B. candida* population dynamics among HSC populations with different characteristics (i.e., abundance and density) may be beneficial for elucidating mechanisms that regulate ectoparasite-host relationships, particularly in such an ancient and stable host species.

Aggregation was observed in the cocoons of *B. candida* in this study as cocoons were significantly more prevalent in the dorsal-most quartile of gill lamellae (Fig. 6). The ventral-most gills were preferentially used for cocoon placement, possibly due to the larger size of these lamellae as larger lamellae size not only provides more habitat, but also allows cocoon locations to be away further from edge of the lamellae, potentially sheltering the cocoons from excessive flow, a critical concern for ectoparasites (Wootten, 1974). Additionally, larger lamellae can pump more water, which may be necessary to meet the oxygen demand of the flatworm cocoons which require oxygen to sclerotize (Huggins & Waite, 1993). It was observed that *B. candida* cocoons were infrequently placed in the CMRA's, a specialized zone of the lamellae important for nitrogenous waste excretion (Henry et al., 1996; Hans et al., 2018). However, we postulate that cocoon placement is fairly random across the CMRA vs. PMPA sections of HSC gills because the CMRA region in this study comprised an average area of 0.30 ± 0.06 SE across the total gill surface while the average proportion of cocoons was 0.21 ± 0.02 SE indicating that the placement of *B. candida* cocoons is nearly proportional to the CMRA. It is important to note that, the CMRA cocoon placement was not entirely avoided in this

study and the likelihood of CMRA cocoon placement appeared to slightly increase with cocoon intensity, albeit, weak relationship between overall cocoon intensity and the proportion of cocoons in the CMRA region. Therefore, it is important to determine if the spatial arrangement (random or clustered) of cocoons on gill lamella is affected across *B. candida* intensity levels in other HSC populations.

The extent of the deleterious impacts imposed by *B. candida* infections remains uncertain; however, HSC physiology could be affected from the combination of anthropogenic and ambient environmental stressors coupled with *B. candida* infection. This study revealed no more than 15% of gill sub-sample surface area in any adult was covered with *B. candida* cocoons, however this estimate is likely conservative as our analysis was unable to detect the cocoon cemented regions with imageJ software (Fig. 5C, D). Additionally, histological analysis identified several areas of gill damage (inflammation, surface defects and hemocyte nodules) further compromising gill function. Lack of non-infected HSCs makes it difficult to confirm with absolute certainty that the gill damage observed in this study is the result of *B. candida* cocoon infections as reported by Leibovitz & Lewbart (2003). Regardless, light infection intensities on gills from ectoparasites may have serious adverse impacts on HSC physiology when coupled with other stressors. For example, ectoparasite coverage on gills appears to be directly proportional to reduction on the velocity of oxygen uptake in aquatic organisms (Duthie & Hughes, 1987) and may reduce respiration efficiency, especially in hypoxic conditions, a problem that is expected to become more chronic and frequent in coastal marine environments in the coming decades (Diaz & Rosenberg, 2008). Moreover, HSCs face a unique and direct anthropogenic stressor in the form of hemolymph extraction for biomedical purposes that may make individuals with intense infections of *B. candida* more susceptible to sublethal effects (i.e., reduced oxygen uptake, increased respiration energy expenditure, etc.) or mortality (Smith et al., 2017; Owings et al., 2019; 2020). The sublethal impacts of biomedical hemolymph extraction on HSC survivors are numerous, such as a significant reduction in hemocyanin concentrations, and reduced spawning frequency (Owings et al., 2019; 2020), and it can take up to 4 months for amebocytes to fully recover to baseline levels (Novitsky, 1984). Therefore, understanding the simultaneous impacts of projected intensifying environmental conditions (i.e., temperature, ocean acidification, and hypoxia), biomedical hemolymph harvest on hemocyanin levels, and *B. candida* infections should be investigated, as their combined effect may engender more severe consequences for HSCs than when these effects are isolated.

Conclusions

This study provides novel insight into *B. candida* infection characteristics across multiple life history stages of *L. polyphemus,* and the results suggest there is a moderate dichotomy of *B. candida* prevalence between instars < 12 and older instars (13 +). This study also demonstrates that cocoon infection intensity and surface area coverage differed substantially in adults, indicating infection is considerably variable. While this work only focused on one *L. polyphemus* population, patterns of *B. candida* infection may not be uniform across all HSC populations. Because parasite abundance can vary due to differences in geographical location, host density, ambient environmental characteristics, and distance between host populations (Poulin et al., 2011), future studies quantifying the *B. candida* intensity and prevalence across other geographically distinct HSC populations are needed. Additionally, other underlying mechanisms (i.e., HSC population density, age group composition, etc.) of *B. candida* infection dynamics should be addressed at the population level to understand both host-parasite ecology and the underpinnings of *B. candida* infection. Based on the findings, overall infection intensity strongly correlates with the 25% ventral-most gill lamellae (Fig. 7) and thus, monitoring programs could expedite intensity enumeration by examining these gill lamellae sections. Considering the vulnerable status of *L. polyphemus* in the U.S., the impact of *B. candida* infection on HSC respiration coupled with environmental stressors should be examined to determine if this host-parasite relationship is contributing to recent population declines.

Acknowledgements The study was partially supported by the National Sea Grant College Program of NOAA to the Research Foundation of State University of New York on behalf of New York Sea Grant and the Ocean and Great Lakes Award through the New York State Department of Environmental

Conservation. We thank Dr. Jan Lovy for providing feedback on Horseshoe-crab gill histology photos, Tom Gariepy from TG Fisheries for providing samples, and Allison Turbush for assisting in data collection. The authors have declared that no competing interests exist.

Funding The Ocean and Great Lakes Award provided by the New York State Department of Environmental Conservation and NOAA New York Sea Grant.

Data availability The datasets and code generated and analyzed during this study are available from the corresponding authors on request.

Declarations

Conflict of interest The authors declare no competing interests.

Ethical approval Organisms and tissue samples collected for this research were permitted through by the New York State Department of Conservation under the Scientific License to Collect #1145 under the New York State Environmental Conservation Law.

References

ASMFC. 2019. 2019 horseshoe crab benchmark stock assessment and peer review report. Arlington, VA, Atlantic States Marine Fisheries Commission.

Bagge, A. M., R. Poulin & E. T. Valtonen, 2004. Fish population size, and not density, as the determining factor of parasite infection: a case study. Parasitology 128(3): 305–313.

Baird, S. F. & C. Girard, 1852. Descriptions of new species of reptiles, collected by the US exploring expedition under the command of Capt. Charles Wilkes, USN: First Part: Including the species from the westerncoast of America. Proceedings of the Academy of natural Sciences of Philadelphia.

Barton, K. & M. K. Barton, 2015. Package 'mumin.' Version 1(18): 439.

Bopp, J. J., M. Sclafani, D. R. Smith, K. McKown, R. Sysak & R. M. Cerrato, 2019. Geographic-specific capture–recapture models reveal contrasting migration and survival rates of adult horseshoe crabs (*Limulus polyphemus*). Estuaries and Coasts 42(6): 1570–1585.

Botton, M. L., 2009. The ecological importance of horseshoe crabs in estuarine and coastal communities: a review and speculative summary, Biology and conservation of horseshoe crabs Springer, Boston, MA: 45–63.

Botton, M. L. & J. W. Ropes, 1987. Populations of horseshoe crabs, *Limulus polyphemus*, on the northwestern Atlantic continental shelf. Fishery Bulletin 85(4): 805–812.

Botton, M. L., Shuster Jr, C.N. & Keinath, J.A., 2003a. Horseshoe crabs in a food web: Who eats whom. The American Horseshoe Crab. Harvard University Press, Cambridge: 133–153

Botton, M. L., R. E. Loveland & A. Tiwari, 2003b. Distribution, abundance, and survivorship of young-of-the-year in a commercially exploited population of horseshoe crabs *Limulus polyphemus*. Marine Ecology Progress Series 265: 175–184.

Brockmann, H. J. & D. Penn, 1992. Male mating tactics in the horseshoe crab *Limulus polyphemus*. Animal Behaviour 44(4): 653–665.

Burnham, K. P. & D. R. Anderson, 2002. A practical information-theoretic approach, Model selection and multimodel inference. Springer, New York.

Carmichael, R. H., D. Rutecki & I. Valiela, 2003. Abundance and population structure of the Atlantic horseshoe crab *Limulus polyphemus* in Pleasant Bay, Cape Cod. Marine Ecology Progress Series 246: 225–239.

Castro, K. M., J. S. Cobb, M. Gomez-Chiarri & M. Tlusty, 2012. Epizootic shell disease in American lobsters *Homarus americanus* in southern New England: past, present and future. Diseases of Aquatic Organisms 100(2): 149–158.

Delignette-Muller, M. L. & C. Dutang, 2015. fitdistrplus: An R package for fitting distributions. Journal of Statistical Software 64(4): 1–34.

Despommier, D.D., Gwadz, R.W. & Hotez, P.J., 2020. Parasitic diseases. Parasites without borders, Inc. Springer. New York: 205–213.

Diaz, R. J. & R. Rosenberg, 2008. Spreading dead zones and consequences for marine ecosystems. Science 321(5891): 926–929.

Drake, A., 2019. Body size predicts the likelihood of harbouring ectoparasites among channel catfish (*Ictalurus punctatus*) in Lac des Chats and its tributaries, University of Ottowa, Ottawa:

Duthie, G. G. & G. M. Hughes, 1987. The effects of reduced gill area and hyperoxia on the oxygen consumption and swimming speed of rainbow trout. Journal of Experimental Biology 127(1): 349–354.

Ebert, D., M. Lipsitch & K. L. Mangin, 2000. The effect of parasites on host population density and extinction: Experimental epidemiology with Daphnia and six microparasites. The American Naturalist 156(5): 459–477.

Estes, M. G., R. H. Carmichael, P. D. Macdonald, A. J. Brady & J. McFadyen, 2015. Molts reveal life-history patterns for juvenile American horseshoe crabs in fringe habitats, Changing global perspectives on horseshoe crab biology, conservation and management Springer, Cham: 255–278.

Eyler, S., 2015. Review of the Atlantic States Marine Fisheries Commission Fishery Management Plan for horseshoe crab, Atlantic States Marine Fisheries Commission, Arlington:

Gaines, E. F., R. H. Carmichael, S. P. Grady & I. Valiela, 2002. Stable isotopic evidence for changing nutritional sources of juvenile horseshoe crabs. The Biological Bulletin 203(2): 228–230.

Galloway, T. D. & R. J. Lamb, 2017. Abundance of chewing lice (*Phthiraptera*: *Amblycera* and *Ischnocera*) increases with the body size of their host woodpeckers and sapsuckers (*Aves*: *Piciformes*: *Picidae*). The Canadian Entomologist 149: 473–481.

Gareth, J., Daniela, W., Trevor, H. and Robert, T., 2013. *An introduction to statistical learning: with applications in R*. Spinger.

Girard, C. 1850. Descriptions of several new species of marine planariae from the coast of Massachusetts. In Proc Boston Soc Nat Hist (Vol. 3, pp. 251–256).

Groff, J. F. & L. Leibovitz, 1982. A gill disease of *Limulus polyphemus* associated with triclad turbellarid worm infections. Biol Bull 163: 392.

Hans, S., Quijada-Rodriguez, A.R., Allen, G.J., Onken, H., Treberg, J.R. and Weihrauch, D., 2018. Ammonia excretion and acid–base regulation in the American horseshoe crab, Limulus polyphemus. *Journal of Experimental Biology*, *221*(6).

Henry, R. P., S. A. Jackson & C. P. Mangum, 1996. Ultrastructure and transport-related enzymes of the gills and coxal gland of the horseshoe crab *Limulus polyphemus*. The Biological Bulletin 191(2): 241–250.

Hudson, P. J., A. P. Dobson & D. Newborn, 1998. Prevention of population cycles by parasite removal. Science 282(5397): 2256–2258.

Huggins, L. G. & J. H. Waite, 1993. Eggshell formation in *Bdelloura candida*, an ectoparasitic turbellarian of the horseshoe crab *Limulus polyphemus*. Journal of Experimental Zoology 265(5): 549–557.

James-Pirri, M. J., K. Tuxbury, S. Marino & S. Koch, 2005. Spawning densities, egg densities, size structure, and movement patterns of spawning horseshoe crabs, *Limulus polyphemus*, within four coastal embayments on Cape Cod, Massachusetts. Estuaries 28(2): 296–313.

Jennings, J. B., 1977. Patterns of nutritional physiology in free-living and symbiotic *Turbellaria* and their implications for the evolution of entoparasitism in the phylum *Platyhelminthes*. Acta Zool Fennica. 154(2): 63–79.

Krøyer, H. E. N. R. I. K. 1837. Om Snyltekrebsene, isaer med Hensyn til den danske Fauna. Naturhistorisk Tidsskrift, 1(2): 172–208.

LaDouceur, E. E., L. Mangus, M. M. Garner & A. N. Cartoceti, 2019. Histologic findings in captive American horseshoe crabs (*Limulus polyphemus*). Veterinary Pathology 56(6): 932–939.

Lauer, D. M. & B. Fried, 1977. Observations on nutrition of *Bdelloura candida* (*Turbellaria*), an ectocommensal of *Limulus polyphemus* (*Xiphosura*). American Midland Naturalist 97: 240–247.

Lehmann, T., 1993. Ectoparasites: direct impact on host fitness. Parasitology Today 9(1): 8–13.

Leibovitz, L. & G. A. Lewbart, 2003. Diseases and symbionts: vulnerability despite tough shells. In Shuster, C. N., R. B. Barlow & H. J. Brockmann (eds), The American Horseshoe Crab Harvard University Press, Cambridge: 245–275.

Linnaeus, C. V. 1758. Systema naturae (Vol. 1).

Loveland, R. E. & M. L. Botton, 1992. Size dimorphism and the mating system in horseshoe crabs *Limulus polyphemis* L. Animal Behaviour 44(5): 907–916.

Lüdecke, Makowski, Waggoner & Patil (2020). Assessment of Regression Models Performance. CRAN. https://easystats.github.io/performance.

Mattei, J. H., M. A. Beekey, A. Rudman & A. Woronik, 2010. Reproductive behavior in horseshoe crabs: Does density matter? Current Zoology 56(5): 634–642.

Milne-Edwards, H., 1837. Élémens de zoologie ou Leçons sur l'anatomie, la physiologie, la classification et les moeurs des animaux. H. Dumont.

Mitchill, S. L. 1814. Natural history. The medical repository of original essays and intelligence, relative to physic, surgery, chemistry, and natural history (1800–1824) 1(4): 396.

Molnar, K., 1994. Effect of decreased water oxygen content on common carp fry with *Dactylogyrus vastator* (*Monogenea*) infection of varying severity. Diseases of Aquatic Organisms 20: 153–153.

Novitsky, T. J., 1984. Discovery to commercialization-the blood of the Horseshoe-crab. Oceanus 27(1): 13–18.

Owings, M., C. Chabot & W. Watson III., 2019. Effects of the biomedical bleeding process on the behavior of the American horseshoe crab, *Limulus polyphemus*, in its natural habitat. The Biological Bulletin 236(3): 207–223.

Owings, M., C. Chabot & W. Watson III., 2020. Effects of the biomedical bleeding process on the behavior and hemocyanin levels of the American horseshoe crab (*Limulus polyphemus*). Fishery Bulletin 118(3): 225.

Pearse, A. S., 1949. Observations on flatworms and nemerteans collected at Beaufort, N. C. Proceedings of the United States National Museum 100: 25–38.

Poulin, R., 2010. Parasite manipulation of host behavior: an update and frequently asked questions, Advances in the Study of Behavior, Vol. 41. Academic Press, Cambridge: 151–186.

Poulin, R., M. E. Rau & M. A. Curtis, 1991. Infection of brook trout fry, *Salvelinus fontinalis*, by ectoparasitic copepods: the role of host behaviour and initial parasite load. Animal Behaviour 41(3): 467–476.

Poulin, R., C. A. Blanar, D. W. Thieltges & D. J. Marcogliese, 2011. The biogeography of parasitism in sticklebacks: distance, habitat differences and the similarity in parasite occurrence and abundance. Ecography 34(4): 540–551.

R Core Development Team. 2020. R: A language and environment for statistical computing. R Foundation for Statistical Computing, Vienna, Austria. https://www.R-project.org/

Riesgo, A., E. A. Burke, C. Laumer & G. Giribet, 2017. Genetic variation and geographic differentiation in the marine triclad *Bdelloura candida* (Platyhelminthes, Tricladida, Maricola), ectocommensal on the American horseshoe crab *Limulus polyphemus*. Marine Biology 164(5): 111.

Rudkin, D. M., G. A. Young & G. S. Nowlan, 2008. The oldest horseshoe crab: a new xiphosurid from Late Ordovician Konservat-Lagerstätten deposits, Manitoba, Canada. Palaeontology 51(1): 1–9.

Rudloe, A., 1981. Aspects of the biology of juvenile horseshoe crabs *Limulus polyphemus*. Bulletin of Marine Science 31(1): 125–133.

Schneider, C. A., W. S. Rasband & K. W. Eliceiri, 2012. NIH Image to ImageJ: 25 years of image analysis. Nature Methods 9(7): 671–675.

Sekiguchi, K., 1988. Biology of horseshoe crabs, Science House, Tokyo:

Shuster, C. N., Jr., 1955. On morphometric and serological relationships within the *Limulidae*, with particular reference to *Limulus polyphemus* (L.), New York University, New York:

Sluys, R. 1989. A monograph of the marine triclads. In Balkema, A. A (ed.), Rotterdam: 463

Smith, D. R., M. J. Millard & R. H. Carmichael, 2009. Comparative status and assessment of *Limulus polyphemus* with emphasis on the New England and Delaware Bay populations, Biology and conservation of horseshoe crabs Springer, Boston: 361–386.

Smith, D. R., M. A. Beekey, H. J. Brockmann, T. L. King, M. J. Millard & J. A. Zaldívar-Rae, 2016. *Limulus polyphemus*. The IUCN Red List of Threatened Species 2016: e.T11987A80159830.

Smith, D. R., H. J. Brockmann, M. A. Beekey, T. L. King, M. J. Millard & J. Zaldivar-Rae, 2017. Conservation status of the American horseshoe crab, (*Limulus polyphemus*): a regional assessment. Reviews in Fish Biology and Fisheries. https://doi.org/10.1007/s11160-016-9461-y.

Stjernman, M., L. Råberg & J. Å. Nilsson, 2008. Maximum host survival at intermediate parasite infection intensities. PLoS One 3(6): e2463.

Tarling, G. A. & J. Cuzin-Roudy, 2008. External parasite infestation depends on moult-frequency and age in Antarctic krill (*Euphausia superba*). Polar Biology 31(2): 121–130.

Taylor, A. C., R. H. Field & P. J. Parslow-Williams, 1996. The effects of Hematodinium sp.-infection on aspects of the respiratory physiology of the Norway lobster, *Nephrops norvegicus* (L.). Journal of Experimental Marine Biology and Ecology 207(1–2): 217–228.

Tompkins, D. M. & M. Begon, 1999. Parasites can regulate wildlife populations. Parasitology Today 15(8): 311–313.

Tsipoura, N. & J. Burger, 1999. Shorebird diet during spring migration stopover on Delaware Bay. Condor. https://doi.org/10.2307/1370193.

Tucker, C. S., C. Sommerville & R. Wootten, 2002. Does size really matter? Effects of fish surface area on the settlement and initial survival of *Lepeophtheirus salmonis*, an ectoparasite of Atlantic salmon Salmo salar. Diseases of Aquatic Organisms 49(2): 145–152.

Walls, E. A., J. Berkson & S. A. Smith, 2002. The horseshoe crab, *Limulus polyphemus*: 200 million years of existence, 100 years of study. Reviews in Fisheries Science 10(1): 39–73.

Watkins, H. V. & G. Blouin-Demers, 2019. Body size, not age, predicts parasite load in Clark's Spiny Lizards (*Sceloporus clarkii*). Canadian Journal of Zoology 97(3): 220–224.

Whittington, I. D., 2005. Monogenea Monopisthocotylea (ectoparasitic flukes). In Rohde, K. (ed), Marine Parasitology CABI, Melbourne: 63–72.

Wootten, R., 1974. The spatial distribution of *Dactylogyrus amphibothrium* on the gills of ruffe Gymnocephalus cernua and its relation to the relative amounts of water passing over the parts of the gills. Journal of Helminthology 48(3): 167–174.